Wiley Online Library
Early View publication on www.wileyonlinelibrary.com
(issue and page numbers not yet assigned;
citable using Digital Object Identifier – DOI)

Phys. Status Solidi A, 1600618 (2017) / DOI 10.1002/pssa.201600618

physica status solidi a
www.pss-a.com
applications and materials science

Influence of the Al content of the AlGaN buffer layer in AlGaN/GaN high-electron-mobility transistor structures on a Si substrate

Yuya Yamaoka*[,1,2], Ken Kakamu[2], Akinori Ubukata[1], Yoshiki Yano[1], Toshiya Tabuchi[1], Koh Matsumoto[1], and Takashi Egawa[2]

[1] Taiyo Nippon Sanso Corporation, 10 Ohkubo, Tsukuba, Ibaraki 300-2611, Japan
[2] Nagoya Institute of Technology, Gokiso-chou, Nagoya, Aichi 466-8555, Japan

Received 14 August 2016, revised 4 January 2017, accepted 5 January 2017
Published online 00 Month 2017

Keywords AlGaN, breakdown voltage, GaN, high electron mobility transistors, silicon, substrates

* Corresponding author: e-mail yuya.yamaoka@tn-sanso.co.jp, Phone: +81 285 29 8246, Fax: +81 3 6866 1511

We investigated the effect of the Al content in the AlGaN buffer layer on the initial AlN nucleation layer, for AlGaN/GaN high-electron-mobility transistors (HEMT), on a Si substrate. Reducing the Al content in the AlGaN layer decreased the surface pit density of the AlGaN layer, and increased the leakage current of the AlGaN/AlN/Si structures, but the crystal quality of the AlGaN layer was not changed by the Al content. The dislocation density of the GaN layer and the two-dimensional electron gas characteristics of the HEMT structures, were almost the same for the AlGaN buffer layer with differing Al content. However, the vertical-direction breakdown voltage (VDBV) was decreased at an Al content of 0.760 compared with other HEMT structures. In addition, the fluctuations of SLS layer were observed at an Al content of 0.760. The warpage and cracking of the HEMT structures were minimized at an Al content of 0.558. Based on these results, the VDBV of HEMT structures are not correlated with the VDBV of the AlGaN buffer layer. However, the VDBV of HEMT structures is affected by the surface pit density of the AlGaN buffer layer. In addition, the warpage of HEMTs on a Si substrate, can be controlled by the Al content of the AlGaN buffer layer.

1 Introduction AlGaN/GaN high-electron-mobility transistors (HEMTs) on large-diameter Si substrates, are expected to help realize low-cost, low-loss, and high-output-power devices [1, 2]. Some device properties, like the maximum output power of the power devices, are determined by the breakdown voltage. The breakdown voltage of lateral devices, such as AlGaN/GaN HEMTs is known to increase as the distance of gate–drain electrodes increases, because the electric field between the gate and drain is decreased. However, Ikeda et al. reported that the lateral breakdown voltage of HEMTs decreases with the vertical-direction breakdown voltage (VDBV), despite the longer distance of gate–drain electrodes [3].

Mechanisms for decreasing the VDBV of AlGaN/GaN HEMTs on a Si substrate have been reported. Umeda et al. demonstrated that the vertical-direction leakage current from inversion electrons at the AlN/Si interface, is prevented by selectively formed p^+ regions in a p-type Si substrate [4]. According to Lu et al., the vertical-direction leakage current has two different mechanisms. The drain-to-substrate forward bias leakage current is due to hole generation in the buffer and electron injection from the Si substrate into the buffer. The source-to-substrate reverse bias breakdown is then due to impact ionization [5]. Zhou et al. proposed that the VDBV is dominated by the space-charge-limited current condition, which involves both acceptor and donor traps in the GaN and buffer layer [6].

The buffer layer of AlGaN/GaN HEMTs on Si substrate consists of GaN, AlGaN, and AlN nucleation layer. It also consists of a strained layer super-lattice (SLS) [7], and a graded AlGaN layer [8] for controlling wafer bowing due to thermal and lattice mismatch stress. The mechanism of the leakage current through the buffer structure is not understood because of this complicated layer structure. Our challenge is to understand the relationship between the

vertical leakage current through the buffer layer, and the crystal quality of each layer in buffer layer. In our previous research, we characterized the AlN nucleation layer to investigate the VDBV of HEMTs [9]. Increasing the screw- or mixed-type dislocation density (DD) in the AlN nucleation layer was found to decrease the VDBV [10]. This result indicates that current leakage occurs through mix- or screw-type dislocations in the high voltage range. In this study, we investigated the relationship between the Al content of the AlGaN layer on the initial AlN nucleation layer (AlGaN buffer layer), and the characteristics of AlGaN/GaN HEMT structures.

2 Experimental Our previous study clearly showed that the crystal quality of the initial AlN nucleation layer affects the VDBV of HEMT structures. In this study, AlN on Si substrates (AlN/Si templates) was used. AlN/Si templates were grown simultaneously using a metalorganic chemical vapor deposition (MOCVD) tool (UR26 K, Taiyo Nippon Sanso Corp., 200 mm × six wafers). The full width at half maximum (FWHM) of the rocking curves of the AlN (002) planes of AlN/Si template was 1227 arcsec. The surface pit density of the AlN/Si template, was $17.5 \times 10^{-9}\,cm^{-2}$. The AlN layer in AlN/Si template was 150 nm thick. All of the samples used in this study were grown on 200 mm wide p-type Si substrates using UR26 K [11]. Trimethylgallium (TMG) and trimethylaluminum (TMA) were used as the group-III sources, and high-purity ammonia (NH_3) was used as the group-V source. Hydrogen and nitrogen were used as carrier gases.

Three types of AlGaN layers were regrown on the AlN templates (single AlGaN layer), to investigate the effect of the Al content in the AlGaN layer on the crystal quality and VDBV of single AlGaN layer. The growth conditions of the single AlGaN layer were constant with the exception of the partial pressure ratio of TMA and TMG. The common growth conditions for the three types were as follows: growth temperature of 940 °C, V/III ratio of 1980, thickness of 250 nm, growth pressure of 13 kPa, and partial pressure of group-III sources of 5.93×10^{-5}. The partial pressure ratios of TMA and TMG (i.e., vapor phase ratio of TMA) for samples A–C were 0.25, 0.50, and 0.75, respectively.

The three types of HEMT structures consisted of the AlGaN barrier layer, AlN spacer, GaN, SLS, and AlGaN buffer layers with thicknesses of 25, 1, 1000, 1800, and 250 nm, respectively. The Al content of the AlGaN barrier layer was 0.23. The SLS layer consists of thin AlGaN and AlN layer. These were regrown from the upper parts of the AlGaN buffer layers on AlN/Si templates. The growth conditions of the AlGaN buffer layer in the three types of HEMT structures were the same as those for the corresponding single AlGaN layer. The partial pressure ratios of TMA and TMG in the AlGaN buffer layer of the HEMT structures were 0.25, 0.50, and 0.75 for samples A′–C′, respectively. The growth conditions of the AlGaN barrier layer, AlN spacer, GaN, and SLS layers were the same for the three types of HEMT structures.

The VDBV was measured for each sample as follows: First, a mesa-like structure was formed by reactive-ion etching. Second, an electrode (Ti/Al/Ni/Au = 15/80/12/40 nm) was fabricated by electron-beam deposition, followed by rapid thermal annealing (N_2 atmosphere, 850 °C, 30 s). The diameter of the electrode was 100 μm. The electrode structure used an ohmic electrode structure for the conventional AlGaN/GaN HEMT [9]. Third, a passivation layer (Al_2O_3 = 20 nm) was deposited by atomic layer deposition (ALD). The passivation layer on the electrode was etched with buffered hydrogen fluoride (BHF; room temperature, 1 min). Finally, the electrode (Ti/Au = 10/150 nm) was deposited to prevent oxidation of the electrode. The VDBV of each sample was measured using a semiconductor parameter analyzer (B1505A, Agilent Technologies).

A scanning electron microscope (SEM; S-4700, Hitachi) was used to compare the surface conditions and layer structures of each sample. An atomic force microscope (AFM; MultiMode™, Veeco) was used to measure the depth of the surface pit of each sample. X-ray diffraction (XRD; D8 DISCOVER, Bruker) was employed to determine the crystal quality of each sample and the Al content in the AlGaN layer. A Hall effect measurement tool (HL5500PC, ACCENT) was used to compare the electron mobility and sheet carrier density of two-dimensional electron gas (2DEG), in the channel of the AlGaN/GaN HEMT structures. The warpage of the HEMT structures was measured by focusing the height of a differential interference contrast microscope (DIC; Nikon, ECLIPSE L200N). The crack length from the wafer edge of the HEMT structures was measured from the DIC image.

3 Characterization of single AlGaN layers on AlN/Si templates Figures 1a–c show SEM images of the surfaces of the single AlGaN layers. The surface pit densities were 0.00×10^{-9}, 0.33×10^{-9}, and $5.64 \times 10^{-9}\,cm^{-2}$ for samples A–C, respectively. The depths of the surface pits were 13 and 31 nm for samples B and C, respectively. The surface pit densities of the single AlGaN layers were less than that of the AlN/Si template. The results indicate that the lateral growth rate of the AlGaN layer increases with the vapor phase ratio of TMG.

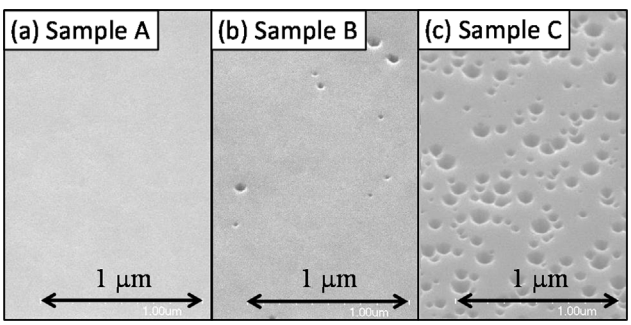

Figure 1 SEM images of the surfaces of a single AlGaN layer on AlN/Si templates for TMA vapor phase ratios of (a) 0.25, (b) 0.50, and (c) 0.75.

The crystal qualities of the single AlGaN layers with various vapor phase ratios of TMA were compared. Figure 2 shows ω-2θ scans for each single AlGaN layer. Because the AlN/Si templates were grown at the same time, the spectral position and FWHM of AlN in each sample matched. The spectral positions of AlGaN in each sample differed because of the changes in the Al content in AlGaN. The FWHMs for the rocking curves of the AlGaN (002) planes and Al content were 1242 arcsec and 0.375 for sample A, 1261 arcsec and 0.558 for sample B, and 1209 arcsec and 0.760 for sample C, while the vapor phase ratios of TMA were 0.25, 0.50, and 0.75, respectively. The crystal quality of the single AlGaN layer did not depend on the vapor phase ratio of TMA. The growth conditions of the single AlGaN layer were the same, except for the vapor phase ratio of TMA.

Figure 3a shows a schematic of the single AlGaN layer structure and the circuit for measuring the vertical leakage current. Figure 3b shows the measurement of the vertical leakage current in the single AlGaN layer structures grown on AlN/Si templates. The leakage current of the single AlGaN layer decreased with the increasing vapor phase ratio of TMA. The VDBVs defined at the leakage current of 1×10^{-6} A mm^{-2} were 18.7, 41.2, and 58.8 V for samples A–C, respectively.

The leakage current can be considered to be affected by the band gap, impurities, and threading dislocations [12] in the material. Khan et al. reported that the band gap of the AlGaN layer increases with the Al content in this layer [13]. The decrease in the leakage current of the single AlGaN structure can be considered to occur with the increasing band gap of the AlGaN layer. However, Nam et al. reported that an Al-rich AlGaN layer is favorable for the formation of deep impurities [14]. Identifying the main cause of the leakage current in a single AlGaN layer structure needs to be investigated while measuring the impurity, and identifying the threading dislocations that form the leakage current path.

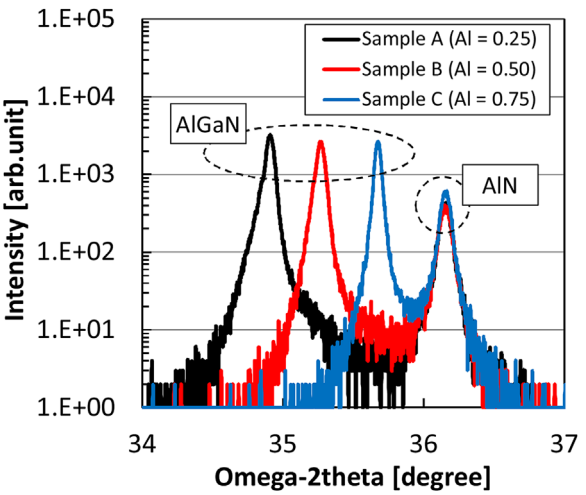

Figure 2 ω-2θ scans for each single AlGaN layer. Note: "Al" in parentheses shows the partial pressure ratios of TMA and TMG in the AlGaN layer of each single AlGaN structure.

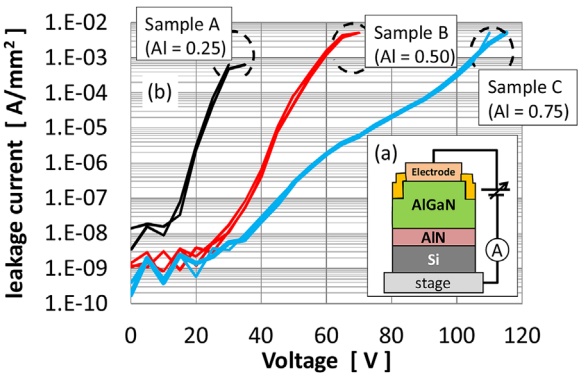

Figure 3 (a) Structure of the single AlGaN layer and the circuit for measuring the vertical leakage current. (b) Current–voltage characteristics of the single AlGaN layer on AlN/Si templates. Note: "Al" in parentheses shows the partial pressure ratios of TMA and TMG in the AlGaN layer of each single AlGaN layer structure.

4 Characterization of HEMT structures on AlN/Si template The crystal quality of the GaN layer, 2DEG characteristics, and warpage in HEMT structures were compared. Table 1 presents the FWHMs of the rocking curves of the GaN (002) and (102) planes, Hall effect measurements of 2DEG at room temperature, and warpage.

The crystal quality of GaN and mobility and sheet carrier density of 2DEG were almost constant and did not depend on the vapor phase ratio of TMA.

The warpage and cracking of HEMT structures were minimized in sample B′. In addition, the warpage of HEMT structures has been reported to be affected by the layer structures and Al or In content in buffer layers [16]. Thus, the warpage of HEMT structures may be controlled by the Al content of the AlGaN buffer layer. The FWHM values of the rocking curve do not depend on the Al content, which suggests the availability of a buffer layer design for future devices on Si substrates.

Figure 4a shows a schematic of the HEMT structure and the circuit for measuring the vertical leakage current. Figure 4b shows the current–voltage characteristics of the HEMT structures regrown on AlN/Si templates. The *I*–*V* curves of samples A′ (vapor phase ratio of TMA in the

Table 1 Characteristics of the HEMT structures.

item	sample A′	sample B′	sample C′
vapor phase ratio of TMA in AlGaN buffer layer	0.25	0.50	0.75
XRD FWHM GaN(002) (arcsec)	584	586	583
XRD FWHM GaN (102) (arcsec)	997	1021	1040
mobility (cm^2 Vs^{-1})	1720	1680	1690
sheet carrier density ($\times 10^{13}$ cm^{-2})	1.16	1.12	1.10
crack length from wafer edge (mm)	0.93	0.09	1.64
warpage (μm)	96	60	170

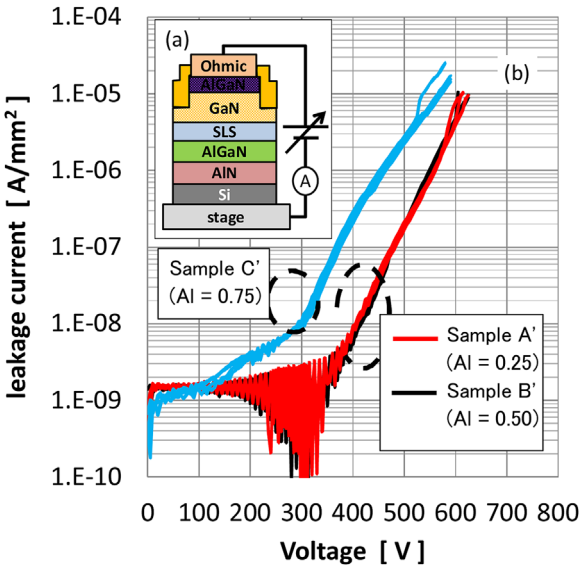

Figure 4 (a) Structure of the HEMT and circuit for measuring the vertical leakage current. (b) Current–voltage characteristics of HEMTs on AlN/Si templates. Note: "Al" in parentheses shows the partial pressure ratios of TMA and TMG in the AlGaN buffer layer of each HEMT structure.

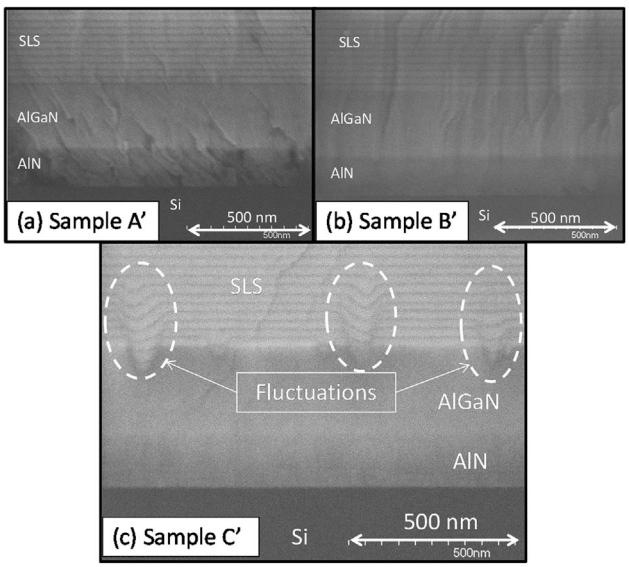

Figure 5 Cross-sectional SEM images of the SLS/AlGaN buffer/AlN/Si substrate interfaces of HEMT structures. The partial pressure ratios of TMA and TMG in the AlGaN buffer layer are (a) 0.25, (b) 0.50, and (c) 0.75.

AlGaN buffer of 0.25) and B′ (vapor phase ratio of TMA in the AlGaN buffer of 0.50) were almost the same. Furthermore, the leakage current of sample C′ (vapor phase ratio of TMA in the AlGaN buffer of 0.75) was increased with other HEMT structures. These results are in contrast to the result for the single AlGaN layer structure (Fig. 3). The thickness of the AlGaN buffer layer in the HEMT structure is less than 10% of the total structure thickness, and both the thickness and Al content of each layer determine the VDBV of the HEMT structures. It is thought that the effect of the VDBV of each AlGaN buffer layer on the HEMT structures is not very strong. The VDBVs of the HEMT structures defined at a leakage current of 1×10^{-6} A mm^{-2} were 550.1, 559.1, and 455.9 V for samples A′–C′, respectively. Therefore, it can be considered that the cause of the decrease in VDBV of sample C′, is a layer other than the AlGaN buffer layer in the HEMT structure on the AlN/Si template.

To study the increased leakage current of Sample C′, a cross-sectional SEM image was used. Figure 5 shows a cross-sectional SEM image of the SLS/AlGaN buffer/AlN/Si substrate interfaces of each HEMT structure. A fluctuation in the interface between the SLS and AlGaN layer was observed for sample C′. As shown in Fig. 1, surface defects, namely V-pits, were generated at the AlGaN surface because lateral growth was affected by Al content. It is thought that some V-pits remained during the growth of SLS and formed threading dislocations. Previous study showed that increasing the thickness of SLS layer increased the VDBV of HEMT structure despite the thickness of the GaN layer [15], and large V-shaped defects in SLS have been correlated with a large gate leakage current in the HEMT structure [17]. Thus, the fluctuation in the interface between the SLS and AlGaN buffer layer can be considered to possibly increase leakage current in the vertical direction of sample C′.

Based on these results, the VDBV of HEMT structures is not correlated with the VDBV of AlGaN buffer layer. However, the VDBV of HEMT structures is affected by the surface pit density of the AlGaN buffer layer, that increases with increasing Al content of the AlGaN buffer layer.

5 Conclusions We investigated the effects of different Al contents on the AlGaN buffer layer using a single AlGaN layer on AlN/Si templates, and AlGaN/GaN HEMT structures on AlN/Si templates.

Decreasing the Al content in the single AlGaN layer decreased the surface pit density and increased the leakage current of the single AlGaN layer. However, the crystal quality of AlGaN layer was not affected by the Al content.

The Al content of the AlGaN buffer layer had no effect on the dislocation density in the GaN layer and 2DEG characteristics of the HEMT structures. However, the VDBV was the lowest at an Al content of 0.760 compared with other HEMT structures. In addition, the fluctuations of the SLS layer were observed at an Al content of 0.760. The warpage and cracking of the HEMT structures were minimized at an Al content of 0.558. Based on these results, reducing the surface pit density of the AlGaN buffer layer could increase the VDBV of HEMT structures. In addition, the warpage of HEMTs on a Si substrate can be controlled by the Al content of the AlGaN buffer layer.

Acknowledgements The authors would like to thank Ms. Chieko Kobayashi and Mr. Kazuhiro Ito for experimental support. This work was supported by the "Aichi Region Super Cluster

Program" of the Ministry of Education, Culture, Sports, Science, and Technology of Japan.

References

[1] D. Christy, T. Egawa, Y. Yano, H. Tokunaga, H. Shimamura, Y. Yamaoka, A. Ubukata, T. Tabuchi, and K. Matsumo, Appl. Phys. Express **6**(2), 026501 (2013).
[2] T. N. Bhat, S. B. Dolmanan, Y. Dikme, H. R. Tan, L. K. Bera, and S. Tripathy, J. Vac. Sci. Technol. B **32**(2) 021206 (2014), DOI: 10.1116/1.4866429
[3] N. Ikeda, Y. Niiyama, H. Kambayashi, Y. Sato, T. Nomura, S. Kato, and S. Yoshida, Proc. IEEE **98**(7), 1151–1161, (2010).
[4] H. Umeda, A. Suzuki, Y. Anda, M. Ishida, T. Ueda, T. Tanaka, and D. Ueda, International Electron Devices Meeting (IEDM10), San Francisco, CA, USA, (2010) pp. 20.5.1–20.5.4, DOI: 10.1109/IEDM.2010.5703400
[5] B. Lu, E. L. Piner, and T. Palacios, Device Research Conference (DRC), Notre Dame, IN, USA, (2010) pp. 193–194, DOI: 10.1109/DRC.2010.5551907
[6] C. Zhou, Q. Jiang, S. Huang, and K. J. Chen, IEEE Electron. Device Lett. **33**(8), 1132–1134 (2012).
[7] S. L. Selvaraj, T. Suzue, and T. Egawa, IEEE Electron. Device Lett. **30**(6), 587–589 (2009).
[8] H. F. Liu, S. B. Dolmanan, L. Zhang, S. J. Chua, D. Z. Chi, M. Heuken, and S. Tripathy, J. Appl. Phys. **113**(2) 023510 (2013).
[9] J. J. Freedsman, A. Watanabe, Y. Yamaoka, T. Kubo, and T. Egawa, Phys. Status Solidi A **213**(2), 424–428, DOI: 10.1002/pssa.201532601 (2016).
[10] Y. Yamaoka, K. Ito, A. Ubukata, T. Tabuchi, K. Matsumoto, and T. Egawa, MRS Adv. **1**(50), 3415–3420 (2016).
[11] Y. Yano, H. Tokunaga, H. Shimamura, Y. Yamaoka, A. Ubukata, T. Tabuchi, and K. Matsumoto, Jpn. J. Appl. Phys. **52**(8S), 08JB06 (2013).
[12] H. Fujiwara, H. Naruoka, M. Konishi, K. Hamada, T. Katsuno, T. Ishikawa, Y. Watanabe, and T. Endo, Appl. Phys. Lett. **100**, 242102, DOI: 10.1073/1.4718527 (2012).
[13] M. R. H. Khan, Y. Koide, H. Itoh, N. Sawaki, and I. Akasaki, Solid State Commun. **60**, 509 (1986).
[14] K. B. Nam, M. L. Nakarmi, J. Y. Lin, and H. X. Jiang, Appl. Phys. Lett. **86**, 222108 (2005).
[15] I. B. Rowena, S. L. Selvaraj, and T. Egawa, IEEE Electron. Device Lett. **32**(11), 1534–1536 (2011).
[16] M. Sasaki, T. Egawa, M. Hao, and H. Ishikawa, Jpn. J. Appl. Phys. **43**(12), 8019–8023 (2004).
[17] T. Narita, A. Wakejima, and T. Egawa, Appl. Phys. Express **9**(3), 031002 (2016).